Ecological Engineering 74 (2014) 290–301

Contents lists available at ScienceDirect

Ecological Engineering

journal homepage: www.elsevier.com/locate/ecoleng

Optimizing nitrate removal and evaluating pollution swapping trade-offs from laboratory denitrification bioreactors

M.G. Healy [a], M. Barrett [b], G.J. Lanigan [c], A. João Serrenho [a], T.G. Ibrahim [c], S.F. Thornton [d], S.A. Rolfe [e], W.E. Huang [f], O. Fenton [c,*]

[a] Civil Engineering, National University of Ireland, Galway, Co., Galway, Ireland
[b] Microbiology, National University of Ireland, Galway, Co., Galway, Ireland
[c] Teagasc, Johnstown Castle, Environment Research Centre, Co., Wexford, Ireland
[d] Groundwater Protection and Restoration Group, Kroto Research Institute, University of Sheffield, UK
[e] Department of Animal and Plant Sciences, University of Sheffield, UK
[f] Kroto Research Institute, University of Sheffield, UK

ARTICLE INFO

Article history:
Received 30 May 2014
Received in revised form 23 September 2014
Accepted 3 October 2014
Available online xxx

Keywords:
Denitrification
Denitrification bioreactors
Greenhouse gas emissions
Pollution swapping

ABSTRACT

Denitrification bioreactors, typically containing woodchips, are artificial sinks used to remediate nitrate (NO_3^-) losses on agricultural landscapes. Analysis of these bioreactors frequently considers their efficacy in terms of only a single contaminant (for example, NO_3^-), but does not consider other losses – ammonium (NH_4^+), phosphorus (PO_4^{3-}), methane (CH_4), carbon dioxide (CO_2) and nitrous oxide (N_2O). In this study, laboratory-scale denitrifying bioreactors operated at hydraulic retention times (HRTs) ranging from 4 to 22 d, containing either lodgepole pine woodchips (LPW), lodgepole pine needles (LPN), barley straw (BBS) or cardboard, were investigated to elucidate operational optima considering three scenarios using: (1) only NO_3^- net fluxes; (2) NO_3^-, NH_4^+ and PO_4^{3-} combined fluxes and (3) all fluxes (water and gaseous) combined. At the end of the experiment, after up to 745 days of operation, the bioreactors were destructively sampled for microbial analysis. In scenario 1, there was a net removal in the bioreactors, which generally performed best at shorter HRTs. In scenario 2, there was a net release of contaminants from all bioreactors, which substantially increased in scenario 3. Total greenhouse gas emissions were highest for the cardboard bioreactors (296 g CO_2-eq m^{-2} d^{-1}) at the longest HRT, and were dominated by CH_4 emissions. Highest N_2O emissions emanated from LPN and LPW bioreactors, which also had a greater proportion of denitrifiers than the other bioreactors. Overall, considering all three scenarios, LPN bioreactors were the best performing at all HRTs. However, the long-term availability of its carbon source may be limited, as there was an 80% reduction over a 560 d period.

1. Introduction

Excess reactive nitrogen, such as nitrate (NO_3^-), ammonium (NH_4^+) or nitrous oxide (N_2O) are now at levels which contribute to eutrophication of terrestrial and aquatic ecosystems (Flechard et al., 2011) and climate change (Richardson et al., 2009). In Europe, nitrogen (N) concentrations in rivers, lakes, aquifers and coastal regions are high in some regions, and groundwater NO_3^- concentrations are generally on the increase (Grizzetti et al., 2012). Residence times of pollutants migrating through soil, subsoil and aquifers can be from months (*e.g.*, well drained and high permeability) to years (*e.g.*, moderately drained and low permeability) (Fenton et al., 2011), leading to sustained losses of NO_3^- to surface water and indirect N_2O emissions to the atmosphere in areas where only partial denitrification occurs (*e.g.*, areas of high water velocity, high dissolved oxygen (DO) concentrations, or low dissolved organic carbon (DOC) concentrations; Durand et al., 2011). The carbon (C) and N cycles are intrinsically linked and depend heavily on the dynamic development of *in situ* microbial communities, which transform these communities *via* different pathways.

Denitrification bioreactors containing organic C rich media, located where denitrification potentials are low and NO_3^- concentrations are high (*e.g.*, drainage tiles or outlets of artificial and natural drainage networks such as pipe and spring outlets), may enhance microbial reduction of NO_3^- by converting it to N_2 (Schipper et al., 2010). Bioreactor design, and in particular hydraulic retention time (HRT), is therefore, important to facilitate

* Corresponding author. Tel.: +353 539171271; fax: +353 53 9171271.
E-mail address: owen.fenton@teagasc.ie (O. Fenton).

http://dx.doi.org/10.1016/j.ecoleng.2014.10.005
0925-8574/

full denitrification, and can be used as a tool to control indirect emissions of N_2O (Fujinuma et al., 2011). These indirect emissions, which may also include losses of other greenhouse gases (GHGs) such as methane (CH_4) and carbon dioxide (CO_2), as well as NH_4^+, phosphorus (P), organic C and metals, is referred to as 'pollution swapping' (Fenton et al., 2014). Relatively few studies have considered pollution swapping in the evaluation of denitrification bioreactors (Grennan et al., 2009; Elgood et al., 2010; Warneke et al., 2011a). However, no study has yet attempted to develop a metric to evaluate the performance of bioreactors containing different C-rich media, which considers pollution swapping across a range of HRTs, and the community of denitrifying micro-organisms supporting this community.

Optimal NO_3^- removal rates ($g\,NO_3\text{-}N\,m^{-3}\,d^{-1}$) depend on factors such as reactive media type, C concentration and bioavailability (Cameron and Schipper, 2010), temperature (Warneke et al., 2011a); hydraulic, DO and NO_3^- loading rates (Grennan et al., 2009; Xu et al., 2009), and HRTs (Chun et al., 2009; Christianson et al., 2011). Typically, optimal N removal rates are determined by operating a bioreactor system under various NO_3^- loading rates (Healy et al., 2006). Fenton et al. (2009) found a direct negative relationship between denitrification potential in shallow groundwater and saturated hydraulic conductivity (k_s) of subsoil. Consequently, even if optimal conditions for denitrification exist (Rivett et al., 2008), microbially-mediated reactions may be limited when k_s, or hydraulic gradients, are too high.

There has been little work on the impact of different C sources on the abundance of the microbial community catalysing NO_3^- removal in denitrifying bioreactors (*e.g.*, Moorman et al., 2010; Warneke et al., 2011b). Warneke et al. (2011b) examined this by measuring the functional gene copy numbers for nitrite reductase, *nirS* and *nirK*, and nitrous-oxide reductase, *nosZ*, for different C substrates, including woodchips, sawdust, green waste, maize cobs and wheat straw, in laboratory bioreactors operated at different temperatures (16.8 and 27.1 °C). They found that microbially-mediated denitrification was the main mechanism for NO_3^--N removal, the abundance of denitrifying genes was similar in all bioreactors operated at the lower temperature, and that NO_3^--N removal was mainly limited by C availability and temperature. No study has yet investigated the development of denitrifying community abundance with respect to distance from the inlet in a denitrifying bioreactor.

The objectives of this study were to: (1) investigate the relationship between NO_3^- removal and pollution swapping during successive, incrementally decreasing HRTs in denitrification bioreactors containing different C-rich media (lodgepole woodchips (LPW), lodgepole pine needles (LPN), barley straw (BBS) and cardboard); (2) identify optimum HRTs for each media, in which acceptable NO_3^- treatment can be achieved, while minimising other losses; and (3) examine whether the source of carbon in a bioreactor influences the abundance of the functional genes *nirK*,*nirS* and *nosZ*.

2. Materials and methods

2.1. Operation of bioreactors

The laboratory bioreactors of Healy et al. (2012) were used in the current study. Briefly, these were 0.1 m-diameter × 1 m-long acrylic columns, which were loaded at the base to allow even saturation and uniform flow into each column. They contained either LPW, cardboard, LPN, or BBS (all at $n = 3$), mixed in alternating 0.03 m-thick layers with soil to give a C source-to-soil volume ratio of 1. Prior to operation, each bioreactor was seeded with approximately 1 L of bulk fluid from a wastewater treatment plant. This fluid was applied to the surface of each bioreactor and allowed to percolate through the media. A control bioreactor ($n = 2$), containing soil only (CSO) was also included. The LPW and cardboard bioreactors were operated to determine their long-term performance. In the Healy et al. (2012) study, all bioreactors were loaded with NO_3^--N solution varying from 19.5 to 32.5 mg L^{-1} at a hydraulic loading rate (HLR) of 3 cm d^{-1}.

In the current study, the bioreactors were operated at incrementally increasing HLRs of 5 and 10 cm d^{-1} (Table 1) and the influent NO_3^--N concentration was varied from 20 to 29.6 mg L^{-1} over both loading rates. A conservative tracer (NaBr, 10 g L^{-1}, applied in one pulse in one constant hydraulic loading interval) was used to estimate the average HRT within each bioreactor, at each HLR, after Levenspiel (1999).

2.2. Water analysis

Water samples collected at the inlet, outlet and at three sampling ports (SPs), located at distances of 0.2 (SP1), 0.4 (SP2) and 0.6 m (SP3) from the inlet of each column, were analysed using standard methods (APHA, 1995) for NO_3^--N, NH_4^+-N, nitrite-N (NO_2^--N), ortho-phosphorus (PO_4^{3-}-P), chemical oxygen demand (COD), pH and DO. Nitrate removal rates (NR; $g\,NO_3^-\text{-}N\,m^{-3}\,d^{-1}$) were calculated taking into account the Darcy velocity (q, $m\,d^{-1}$), cross sectional area (A, m^2), volume of the active area of the bioreactors (m^3), and change in NO_3^--N concentration from the inlet to outlet ($\Delta[NO_3^-\text{-}N]$, $g\,m^{-3}$):

$$NR = \frac{q \times A \times \Delta[NO_3^- - N]}{\text{media volume}} \left(gNO_3^- - N m^{-3} d^{-1}\right) \quad (1)$$

2.3. Greenhouse gas analysis

The emission of GHG, comprising CO_2, CH_4 and N_2O, from each column was measured at specific times at each HLR using the static

Table 1
Media used in denitrification bioreactors, period of operation (d), hydraulic retention time (HRT; d), nitrate (NO_3^--N) removal (expressed as difference between inlet and outlet concentration; %) at each hydraulic loading rate (3, 5, and 10 cm d^{-1}) applied to the bioreactors.

Media[a]	Column	HLR (cm d^{-1})			HLR (cm d^{-1})			HLR (cm d^{-1})[b]		
		3	5	10	3	5	10	3	5	10
		Period of operation (d)			HRT (d)			NO_3-N removal		
LPW	1	460	238	47	17.4	7.7	4.9	99.6	82.6	58.8
	2				13.0	8.1	3.7	99.6	93.1	57.7
	3				14.8	9.2	5.7	99.7	99.4	77.2
–										
Cardboard	1	438	237	47	10.2	6.7	4.0	99.7	99.5	99.7
	2				8.5	7.4	4.8	99.5	99.4	99.7
	3				10.9	6.9	3.5	99.8	99.4	99.7
–										
LPN	1	278	237	47	9.9	9.6	4	99.8	99.4	99.7
	2				11.6	6.7	4	99.7	99.2	99.7
	3				9.9	9.5	3.6	99.9	99.4	99.7
–										
BBS	1	231	133	47	13.9	7.0	3.5	–	99.4	99.7
	2				21.7	8.8	3.9	–	99.7	99.7
	3				18.2	7.3	3.6	–	99.5	99.7
–										
Soil	1	257	134	47	15.5	6.1	4.6	16.5	4.6	−1.4
	2				11.8	6.4	3.8	28.0	0.9	−0.4

[a] LPW = lodgepole pine woodchips; LPN = lodgewood pine needles; and BBS = barley straw.
[b] Nitrate removal and efficiency reported at steady-state only. Steady-state was not attained at a HLR of 3 cm a HLR of 3 cm d^{-1} for BBS (Healy et al., 2012).

chamber technique (Hutchinson and Mosier, 1981). The headspace above each column was flushed with argon (Ar) gas for 5 min at a flow rate of 3 L min^{-1}. Gas samples were withdrawn at 0, 15 and 30 min, and samples were analysed using a gas chromatograph (GC) (Varian GC 450; The Netherlands) and automatic sampler (Combi-PAL autosampler; CTC Analytics, Zwingen, Switzerland). Fluxes of CO_2, CH_4 and N_2O for each chamber were measured as a function of headspace gas accumulation over time (Hutchinson and Mosier, 1981). Data analyses were performed on average daily and cumulative emissions by ANOVA, using the PROC GLM procedure of SAS (SAS Institute, Cary, NC, 2003) with *post-hoc* least significant differences (LSD) tests used to identify differences between treatments.

2.4. Carbon, nitrogen and phosphorus analysis of soil and media

Before construction of the bioreactors, the C and N content of all C-rich media and soil were determined using a thermal conductivity detector, following combustion and separation in a chromatographic column, and the P content was determined by inductively coupled plasma emission spectroscopy (ICP-ES) after aqua regia digestion. As the C-rich media were placed in the bioreactors in alternating 0.03 m-thick layers with soil and the total mass within each reactor was measured, the initial C and N content, expressed as %w/w, and the P content, expressed as mg kg^{-1} (dry matter), in each bioreactor could be calculated. Upon completion of the experiment, two denitrifying bioreactors from each treatment were destructively sampled and samples from four sections, each 0.2 m in length, of each bioreactor (inlet to SP1, SP1–SP2, SP2–SP3, SP3–SP4) were analysed for C, N and P content. This enabled the relationship between total C loss within each bioreactor and the cumulative COD loss, the C content of the bioreactors, and the loss of P to be deduced for the period of operation.

2.5. DNA extraction and real-time PCR analysis on the media

Real time PCR was used to quantify the archaeal and bacterial 16S rRNA populations present in each bioreactor, as well as populations of denitrifying microorganisms using the denitrifying genes, *nirK*, *nirS* and *nosZ* (Table 2). Archaeal and bacterial 16S rRNA populations were distinguished by using two sets of primers and specific probes for each group. Results are described as gene copy concentrations per gram of soil (GCCs/GCs $g_{[soil]}^{-1}$).

Soil used for microbiological analysis was sampled from each 0.2-m-length of each column (inlet to SP1, SP1–SP2, SP2–SP3, SP3–SP4), and the genomic DNA was extracted from 0.5 g/soil using the UltraClean™ Soil DNA Isolation kit following the manufacturer's guidelines. The extracted genomic DNA was visualized on 1% (w/v) 1X TAE agarose gels and was quantified using the Nanodrop 2000c spectrophotometer (Thermo Scientific Inc.). Extracted DNA was then stored at −20 °C.

Standard curves for absolute quantification of archaeal and bacterial 16S rRNA genes and the *nirS*, *nirK* and *nosZ* denitrification genes were constructed using the corresponding standard strains and primer/probe sets outlined in Barrett et al. (2013) (Table 2). Briefly, a 10-fold dilution series of each standard plasmid solution was prepared and analysed using the Light Cycler 480 (Roche, Mannheim, Germany); real-time PCR was carried out in duplicate employing the corresponding primer/probe set outlined in Yu et al. (2005) and Barrett et al. (2013). For the archaeal 16S rRNA gene, an equimolar mixture of the corresponding standard plasmids was used as the template solution for construction of the standard curve (Yu et al., 2005; Lee et al., 2009). Bacterial and archaeal 16S rRNA genes were analysed in duplicate using the Light Cycler 480 (Roche, Mannheim, Germany), the LightCycler 480 Taqman hydrolysis probe Master kit (Roche), and the corresponding primer/probe sets and LightCycler 480 Probe Master kit (Roche; Table 2). The *nirK*, *nirS* and *nosZ* genes were analysed using the corresponding primer sets with the LightCycler 480 SYBR Green I Master kit (Roche), in a total volume of 20 μL, according to the manufacturer's instructions (Yu et al., 2005; Barrett et al., 2013). The thermal cycling protocol was as outlined in Braker et al. (1998), Kandeler et al. (2006) and Henry et al. (2006).

Changes in gene copy number between all samples generated from replicate bioreactors and sampling ports using alternative C sources were analysed with one-way ANOVA, followed by the *post-hoc* Tukey test (Graph Pad InStat V3). Individual regression analysis of *nirK* and *nirS* gene copy number versus N_2O as for *nosZ* and N_2 were also carried out using Graph Pad InStat V3. Using Primer v6 (Primer-E, Plymouth, UK), a Bray-Curtis resemblance matrix (Clarke et al., 2006) was generated for each bioreactor and sampling port using square root transformed mean 16S rRNA, *nirS*, *nirK* and *nosZ* gene copy abundances. Using the resultant resemblance matrix, the data were analyzed in a group average hierarchical cluster dendrogram.

2.6. Sustainability index

Fenton et al. (2014) developed a simple method to quantify the effectiveness of denitrification bioreactors, which considered 'pollution swapping'. In this method, the removal or production

Table 2
Realtime primer and probes for microbial analysis (adapted from Barrett et al., 2013).

Gene	Standard strains	Oligoneucleotidea[e]	Sequences (5′–3′)	Amplicon size (bp)	References
nirS	*Pseudomonas Stutzeri* ATCC 14,405[a]	F: *nirS*Cd3aF	AACGYSAAGGARACSGG	425	Kandeler et al. (2006)
		R: *nirS*R3cd	GASTTCGGRTGSGTCTTSAYGAA		
nirK	*Alcalignes* species DSMZ 30,128[b]	F: nirk 1F	GG(A/C) ATG GT (G/T) CC(C/G) TGG CA	514	Braker et al. (1998)
		R: nirk 5R	GCC TCG ATC AG (A/G) TT(A/G) TGG		
nosZ	*Bradyrhizobum Japonicum* USDA 110[c]	F: *nosz* 2F	CG(C/T)TGTTC(A/C)TCGACAGCCAG	267	Henry et al. (2006)
		R: *nosz* 2R	CAKRTGCAKSGCRTGGCAGAA		
Bacterial 16S rRNA	*Escherichia coli* K12[d]	F: BAC 338F	ACTCCTACGG GAGGCAG	466	Yu et al. (2005)
		R: BAC 805R	GACTACCAGGGTATCTAATCC		
		P: BAC516F	TGC CAG CAG CCG CGG TAA TAC		
Archaeal 16S rRNA		F: ARC787	ATTAG ATACC CSBGT AGTCC AGGAA TTGGC	273	Yu et al. (2005)
		R: ARC1059	GGGGG AGCAC		
		P: ARC915	GCCAT GCACC WCCTC T		

[a] ATCC: American type culture collection.
[b] DSMZ: The German Resource Centre for Biological Material.
[c] USDA: United States Department of Agriculture.
[d] Gift.
[e] P: TaqMan probe; F: forward primer; and R: reverse primer.

of each measured parameter is considered separately. To create equivalence between water and gas measurements, all parameters are expressed in $g\,m^{-2}$ (of bioreactor surface area) d^{-1} and the GHGs are expressed in CO_2 equivalents to account for global warming potential. Negative and positive balances of each parameter indicate either removal or production of the parameter of interest. A sustainability index (SI) is then created by adding each of these parameters together, after Fenton et al. (2014):

$$SI = a(B_{N_2O}) + b\left(B_{NO_3^-}\right) + c(B_{CH_4}) + d(B_{CO_2}) + \text{etc}\ldots \quad (2)$$

where B_x denotes the net flux (either positive or negative) of a specific parameter (x) from the denitrification bioreactor, and *a*, *b*, *c*, etc. are weighting factors that depend on the context of the analysis (*e.g.*, legislative, environmental, geographical). For example, if NO_3^- was considered the most important parameter, the weighting factor b in Eq. (2) would be set at 1 and all other parameters would be less than 1. Three simple scenarios are considered in this study – scenario 1: in countries where NO_3^- removal is of most interest and GHG emissions to the atmosphere are perceived as secondary, the weighting factor for NO_3^- is set to 1 and those for the other measured parameters (NH_4^+-N, PO_4^{3-}-P, CH_4, CO_2 and N_2O) are set to zero; scenario 2: in countries where legislative drivers are focused on water quality and losses of GHG to

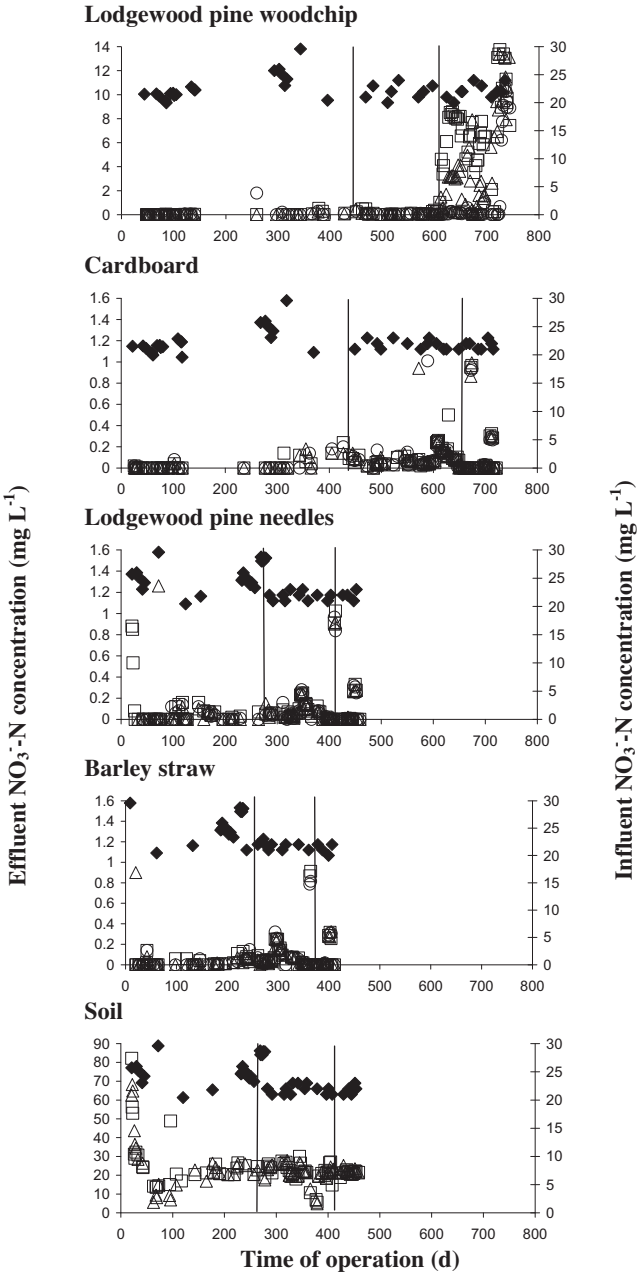

Fig. 1. Influent and effluent nitrate concentrations and operation boundaries for each media. Open square = column 1 effluent; open triangle = column 2 effluent; open circle = column 3 effluent; closed diamond = influent NO_3^--N concentration. Vertical lines represent the three hydraulic loading rates: 3, 5 and 10 cm d^{-1}.

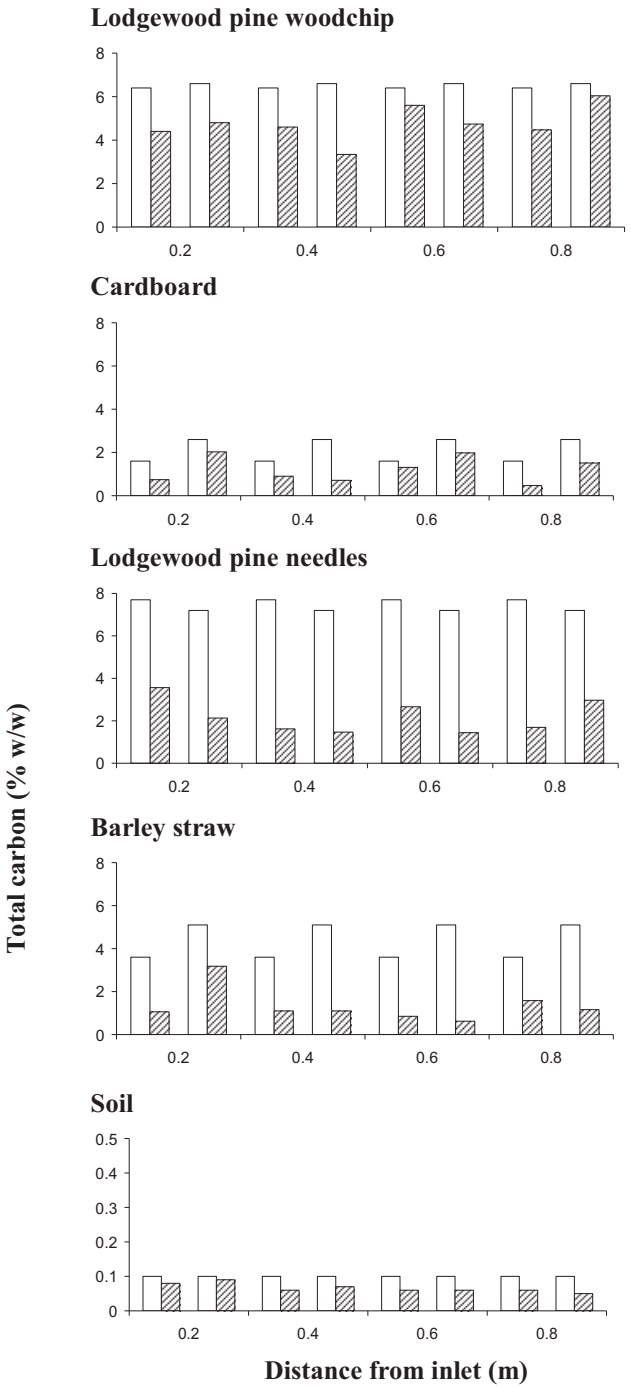

Fig. 2. Total carbon, expressed as a % of total carbon per dry weight of material (soil + filter media) in each 0.2 m depth of the bioreactors ($n = 2$) at the start and end of the study. White boxes = total carbon (%w/w) at the start of the study. Hatched boxes = total carbon (%w/w) at the end of the study.

the atmosphere are considered less important, appropriate weighing factors are applied to NO_3^-, PO_4^+ and NH_4^+; GHGs are not considered and are set to zero. Taking Ireland as an example, the maximum admissible concentration (MAC) for molybdate-reactive phosphorus (MRP = PO_4^{3-}-P in the current study) and NH_4^+ in rivers is 35 μg P L^{-1} and 65 μg N L^{-1}, respectively, while NO_3^- in groundwater should not exceed 8.47 mg N L^{-1} (the current threshold, whereas 11.3 mg N L^{-1} is the MAC). As PO_4^{3-}-P is the most sensitive parameter in this case, the weighting factors for PO_4^{3-}-P, NH_4^+-N and NO_3-N are set to 1, 0.538 (35/65) and 0.004 (35/847), respectively; scenario 3: gaseous and water emissions are considered. Here, the weighting factor for CO_2, CH_4 and N_2O is set at 1, 25 and 296, respectively, and is expressed in CO_2 equivalents (IPCC, 2013). A scoring system was used across the three scenarios, with the best performing media assigned the lowest score. This methodology is very much a preliminary approach as to how a SI may be developed. However, it provides a framework to which a more nuanced holistic analysis of the performance of a bioreactor may be performed.

3. Results

3.1. Removals within each media type

The influent and effluent NO_3^--N concentrations in all bioreactors at the three HLRs examined are illustrated in Fig. 1. For all HLRs the N removal, expressed in terms of influent and effluent NO_3^--N concentrations (single contaminant approach) in the cardboard, LPN and BBS bioreactors, were above 99.4%. The LPW and the cardboard bioreactors had comparable NO_3^--N removals to the other bioreactors during the first and second HLRs, but both had average removals of 57.7–77.2% for a HLR of 10 cm d^{-1}. The ratio of C lost from the LPW bioreactors over their total period of operation (Fig. 2) to the N loading on the bioreactors was, on average, 22:1 – higher than the optimal ratio of around 10:1 for the occurrence of denitrification (Henze et al., 1997). This means that denitrification was not limited by C availability (bioavailability of carbon was not measured in the current study). This suggests that another process was causing the poor NO_3^--N removal. This may have been the HRT (Fig. 3), as one set of LPW bioreactors with an average HRT of 3.7 d (the lowest HRT measured in the study) had low NO_3^--N removals. However, LPW bioreactors performed well at a HRT of 4.9 d (Fig. 3). At the end of the experiment, all bioreactors were operated for 28 d at the first HLR (3 cm d^{-1}) to determine if the HRT limited their performance. During this time, the bioreactors returned to almost 100% NO_3^--N removal (single contaminant approach, results not shown), which confirmed that bioreactors should be operated at a HRT of between 5 and 10 d for optimal NO_3^--N removal (assuming operational temperature, bioreactor construction and influent concentrations are similar to this study).

The bioreactors containing LPN had a large initial release of COD (up to 5000 mg L^{-1}), which lasted for approximately 200 days of operation (Fig. 4). During this period, up to 80% of the total carbon at each depth increment was lost from the LPN bioreactors (Fig. 2).

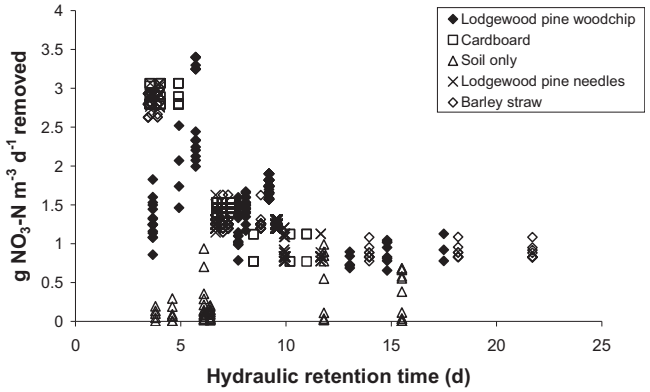

Fig. 3. Relationship between hydraulic retention time (d) and nitrate-N removed (g NO_3-N m^{-3} d^{-1}).

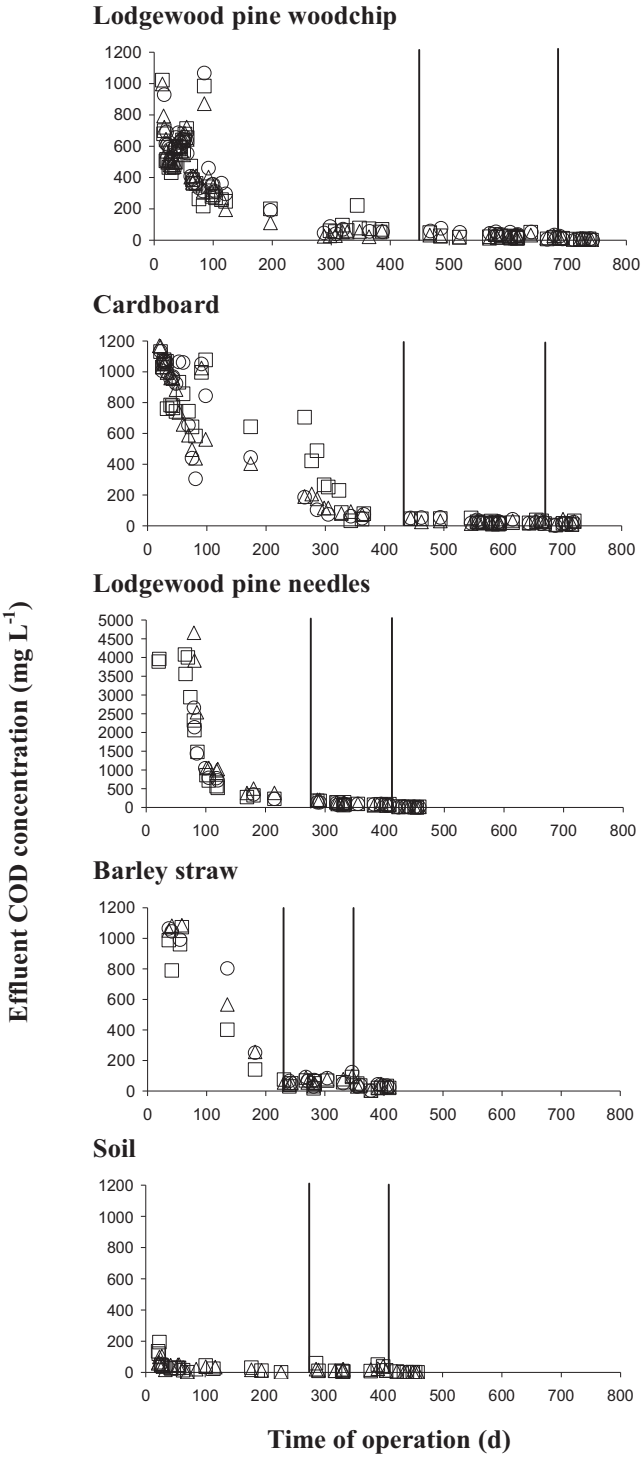

Fig. 4. Effluent COD concentrations and operation boundaries for each media. Open square = column 1; open triangle = column 2; open circle = column 3. Vertical lines represent the three hydraulic loading rates: 3, 5 and 10 cm d^{-1}.

The results from all bioreactors indicate that there is a strong relationship ($R^2 = 0.73$) between the % of total carbon loss and cumulative COD released, according to the following equation:

$$\text{Cumulative COD release(g)} = 5.77 \times \text{TC loss(\%)} - 3.4 \quad (3)$$

Most of the NO_3^- removal occurred within 0.4–0.6 m from the inlet of all bioreactors (Fig. 5) for all the HLRs examined. This suggests that, excluding LPW bioreactors, there may have been some capacity to reduce the HRT without adversely affecting system performance. This is supported by Fig. 3, which indicates that, with the exception of LPW bioreactors (whose performance reduced below a HRT of 4.9 d), NO_3^--N removal increased with decreasing HRT. Although there was an initial release of NH_4^+-N after system start up (Fig. 6), with the exception of the LPW bioreactors, there was no significant release of NH_4^+-N at any depth increment within the bioreactors (Fig. 7). This indicates that dissimilatory nitrate reduction to ammonium (DNRA), or any other microbially-mediated process, may either have only occurred at bioreactors start up when highly reducing conditions existed and when there was less dilution of the released NH_4^+-N.

Although the LPW had a P content of 41.9 mg kg^{-1} (the lowest of all the media examined; Healy et al., 2012), it had the highest concentration of PO_4^{3-}-P (1.1 mg PO_4^{3-}-P L^{-1}) in the final effluent (Fig. 8). (Cardboard had a P content of 96.1 mg kg^{-1} and also had a final effluent concentration close to 1 mg PO_4^{3-}-P L^{-1}). However, in both cases, elevated P release occurred at the start of operation (at 3 cm d^{-1}). For all media tested, the P content of the bioreactors did not change much from their initial P content (calculated per weight of soil and media mixture; results not shown). This indicates that the P was relatively immobile and, even under anaerobic conditions, P was not released from the bioreactors in large amounts.

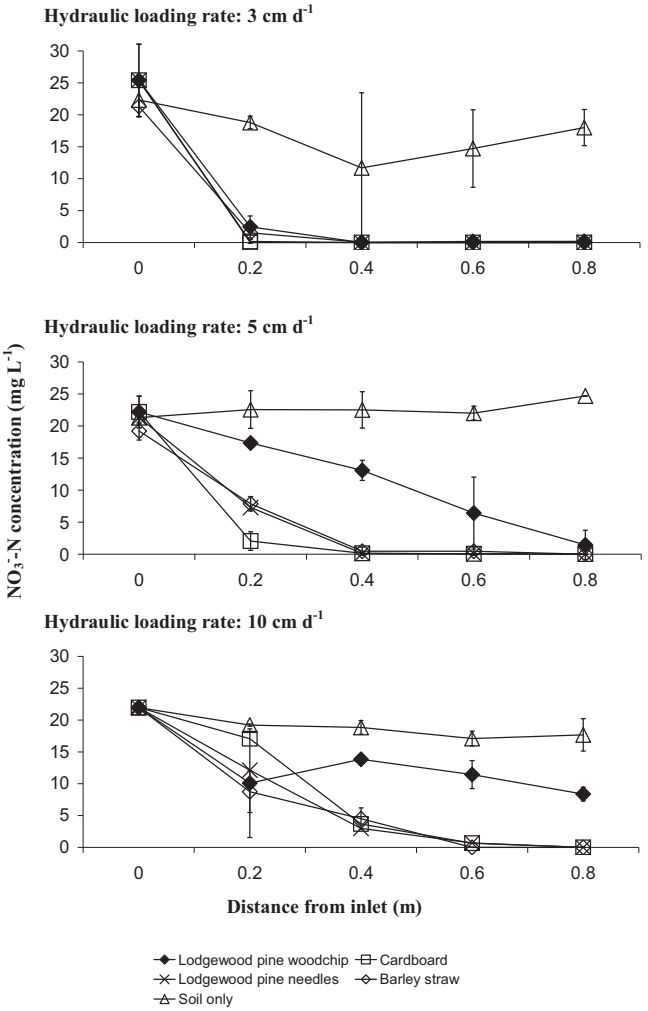

Fig. 5. Average concentration of nitrate in one representative bioreactor containing each media during operation at hydraulic loading rates of 3, 5 and 10 cm d^{-1}.

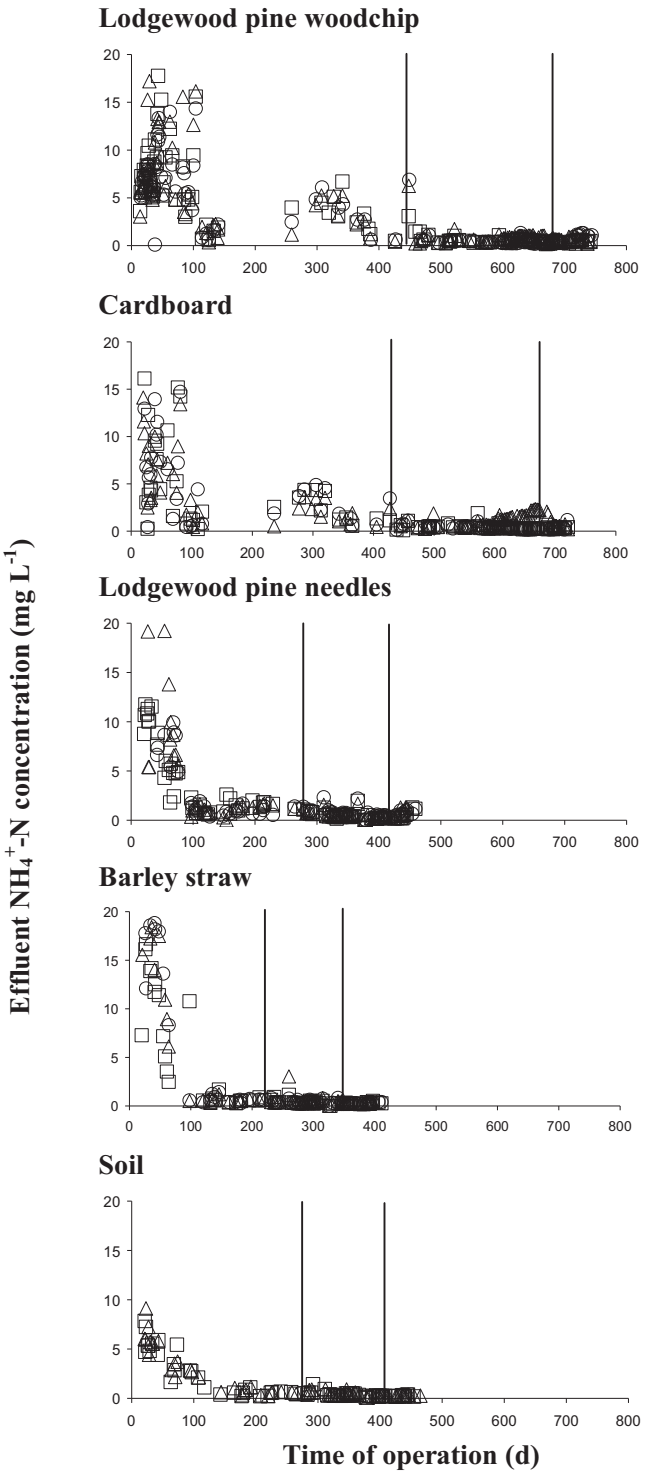

Fig. 6. Effluent ammonium-N concentrations and operation boundaries for each media. Open square = column 1; open triangle = column 2; open circle = column 3. Vertical lines represent the three hydraulic loading rates: 3, 5 and 10 cm d^{-1}.

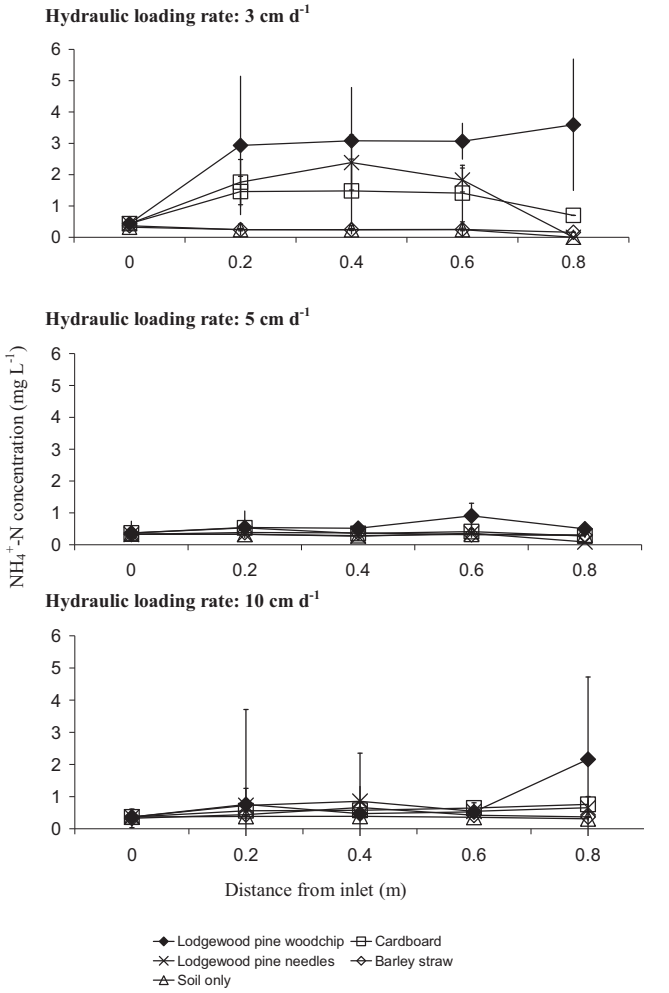

Fig. 7. Average concentration of ammonium-N in one representative bioreactor containing each media during operation at hydraulic loading rates of 3, 5 and 10 cm d^{-1}.

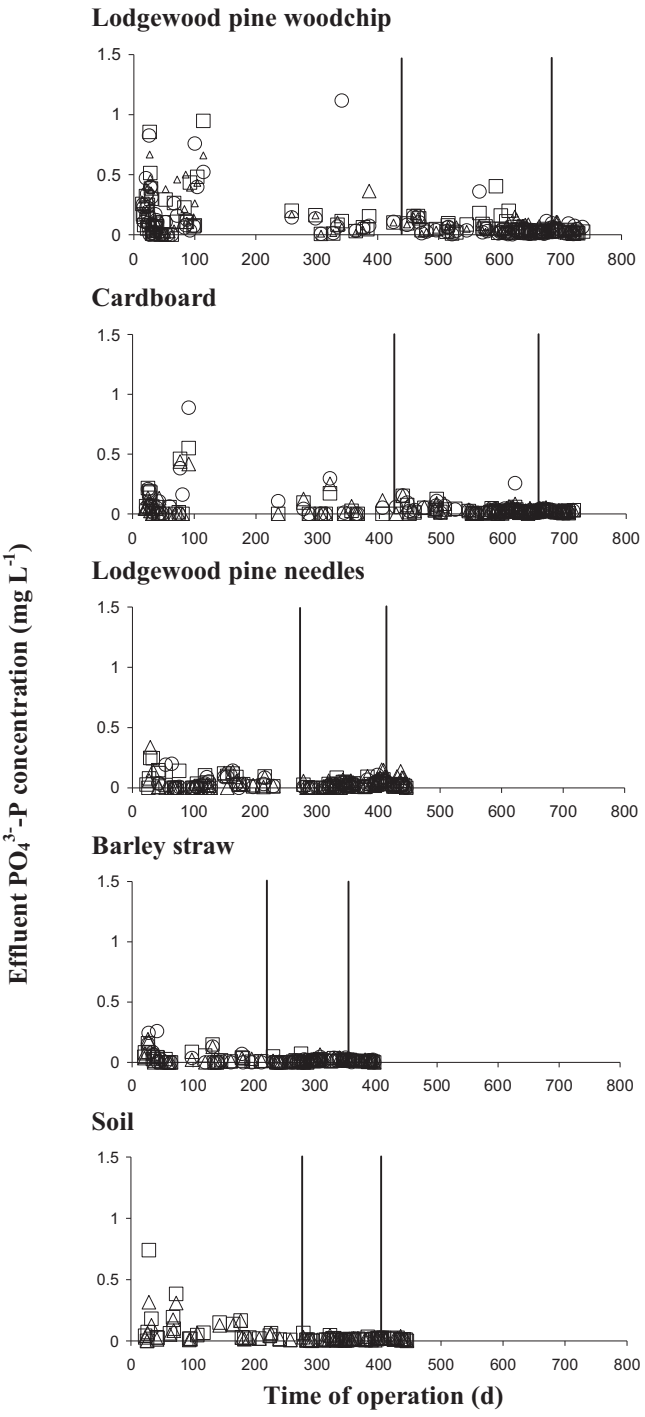

Fig. 8. Effluent ortho-phosphorus concentration and operation boundaries for each media. Open square = column 1; open triangle = column 2; open circle = column 3. Vertical lines represent the three hydraulic loading rates: 3, 5 and 10 cm d^{-1}.

3.2. Greenhouse gas emissions

Mean daily GHG emissions associated with different media are shown in Fig. 9. Nitrous oxide emissions were generally extremely low, ranging from 0.04 to 8.8 mg N_2O-N m^{-2} d^{-1}. With the exception of the CSO and BBS bioreactors (where emissions never rose above 0.4 mg N_2O-N m^{-2} d^{-1}), the highest N_2O emissions occurred at the highest loading rate (Fig. 10), with fluxes of 1.48, 7.1 and 8.8 mg N_2O-N m^{-2} d^{-1} for cardboard, LPW and LPN, respectively. Methane emissions ranged from 0.04 mg CH_4-C m^{-2} d^{-1} in the CSO bioreactors at the 10 cm d^{-1} loading rate to 8.9 g CH_4-C m^{-2} d^{-1} for cardboard at the 3 cm d^{-1} loading rate. Emissions from the BBS bioreactors were also high at the lowest loading rate (3.0 g CH_4-C m^{-2} d^{-1}). Indeed, with the exception of LPW and LPN bioreactors, the highest mean daily CH_4-C emission rate for all media occurred at the lowest loading rate (Fig. 10). A similar emissions pattern is evident for CO_2, with the highest observed flux for cardboard and BBS bioreactors at the 3 cm d^{-1} loading rate (5.7 g CO_2-C m^{-2} d^{-1} and 2.25 g CO_2-C m^{-2} d^{-1}, respectively). The CO_2 rates for the CSO bioreactors were consistently the lowest for all loading rates (Fig. 10).

In terms of global warming potential (GWP), GHG fluxes were dominated by CH_4 emissions (Fig. 9). This is because the GWP of CH_4 is 25 times higher than CO_2, even though the fluxes were similar in terms of the mass of C released. Total GHG fluxes ranged from >0.1 g CO_2-eq m^{-2} d^{-1} for the soil control to 296 g CO_2-eq m^{-2} d^{-1} for CCB at the lowest loading rate (Fig. 9). Emissions from CCB varied from 85 to 296 g CO_2-eq m^{-2} d^{-1}, over 50 times higher than for all other media, with the exception of BBS at the 2 cm d^{-1} and 5 cm d^{-1} loading rates (Fig. 9).

3.3. Microbiological results

Using one-way ANOVA, GCCs appeared to vary significantly within the bioreactors ($P < 0.0001$). The bacterial GCCs recorded

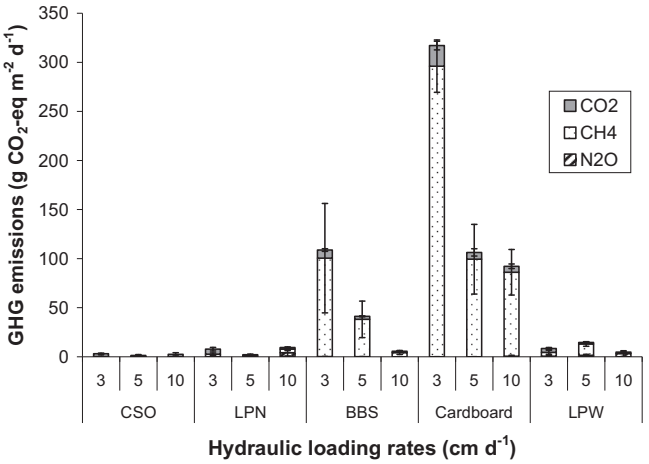

Fig. 9. Mean emissions of greenhouse gas (nitrous oxide (N_2O), methane (CH_4) and carbon dioxide (CO_2)) emissions (±standard error), expressed as CO_2 equivalents per unit surface area per day.

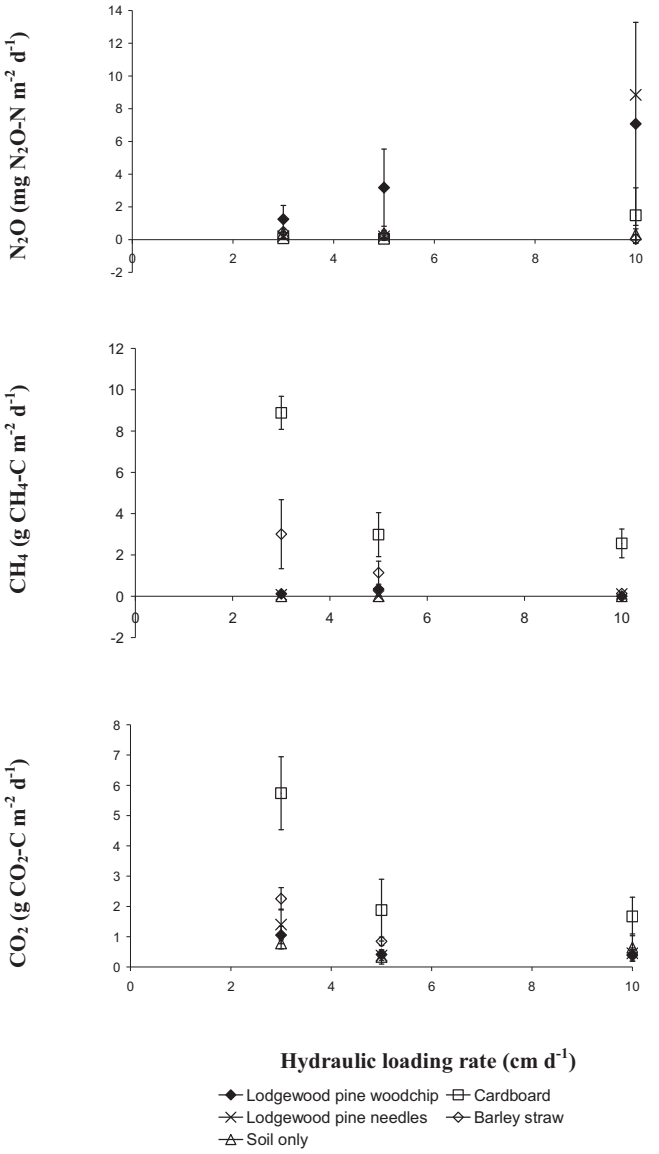

Fig. 10. Relationship between hydraulic loading rate and emissions (±standard error) in the denitrifying bioreactors.

varied significantly ($P = 0.0008$), with the bacterial GCCs from the cardboard bioreactors considerably greater than all other bioreactors ($P < 0.05$). Archaeal GCCs varied significantly between the bioreactors and sampling ports ($P = 0.0049$; Fig. 11). The abundance of the denitrifying genes *nirS*, *nirK* and *nosZ* was significantly different in all bioreactors ($P = 0.0303$; $P = 0.0054$; $P = 0.0043$). The most abundant denitrifying gene was *nirS*, for which the highest GCCs were recorded 0.2 m from the inlet of the cardboard bioreactor (1.32×10^8 GCC g^{-1} dry substrate). *NirS* GCCs from the cardboard bioreactors were significantly greater than the CSO bioreactors ($P < 0.05$). Overall, recorded *nirS* GCCs were greater than *nirK* GCCs. The *nirK* GCCs in the cardboard bioreactors were significantly higher than the CSO, LPN and LPW bioreactors ($P < 0.05$; $P < 0.05$; $P < 0.05$). The *nosZ* GCCs in the cardboard bioreactors were also significantly greater than the CSO, BBS and LPN bioreactors ($P < 0.01$; $P < 0.05$; $P < 0.05$). Using Primer v6, a Bray–Curtis resemblance matrix was generated for each bioreactor and sampling port using square root transformed mean 16S rRNA, *nirS*, *nirK* and *nosZ* gene copy abundances. The resultant resemblance matrices from the Bray–Curtis analysis of the total and denitrifying bacterial communities (from molecular data) showed that there was clustering between sampling ports from each bioreactor, i.e., CSO bioreactors display a 90–100% similarity between its sampling ports (results not shown). The LPN and LPW bioreactor sampling ports were clustered together and had an 80–90% similarity, whereas the CSO and cardboard bioreactors displayed a 60–70% similarity.

4. Discussion

4.1. Nitrate removal

The maximum NO_3^--N removal rate measured was approximately 3.5 g NO_3^--N m^{-3} d^{-1}, which is similar to other laboratory studies using wood-based media (*e.g.*, 1.3–6.2 g NO_3^--N m^{-3} d^{-1}, Warneke et al., 2011b; 3.9 g NO_3^--N m^{-3} d^{-1}, Grennan et al., 2009; 3.4 g NO_3^--N m^{-3} d^{-1}, Schmidt and Clark, 2012), but much lower than some studies using wood-based media (*e.g.*, Robertson, 2010). Although the total carbon content and the ratio of C lost from the bioreactors over their total period of operation to the N loading on the bioreactors was adequate to sustain denitrification, the bioavailability of C was not measured. Other methods may be used to assess the denitrification potential of bioreactor media, such as Schmidt and Clark (2013), who assessed the long-term denitrification potential of various media by calculating the effluent DOC load (in g DOC m^{-3} of media per day) over time. It is unlikely that NO_3^--N removal rates were limited by the influent NO_3^--N concentration, which was between 19.5 and 32.5 mg L^{-1}, or by the slow reaction kinetics in the conversion of NO_3^- to N_2, as NO_3^--N removals increased with reducing HRT. However, bioreactor performance may have been affected by the operational temperature (10 °C), as shown in other studies (Cameron and Schipper, 2010; Warneke et al., 2011b).

Nitrite reductase genes (*nirS* and *nirK*) ranged from 10^4 to 10^7 GCC g^{-1} dry substrate in this study (Fig. 11), which is in the same range measured by Warneke et al. (2011b). As the NH_4^+-N concentration at the outlet from all bioreactors was generally low, it is unlikely that DNRA contributed significantly to NO_3^--N removal. This indicates that denitrification was most likely the main mechanism for NO_3^--N removal, the extent of which was affected by the bioreactor HRT (Fig. 3). The pH measured along the

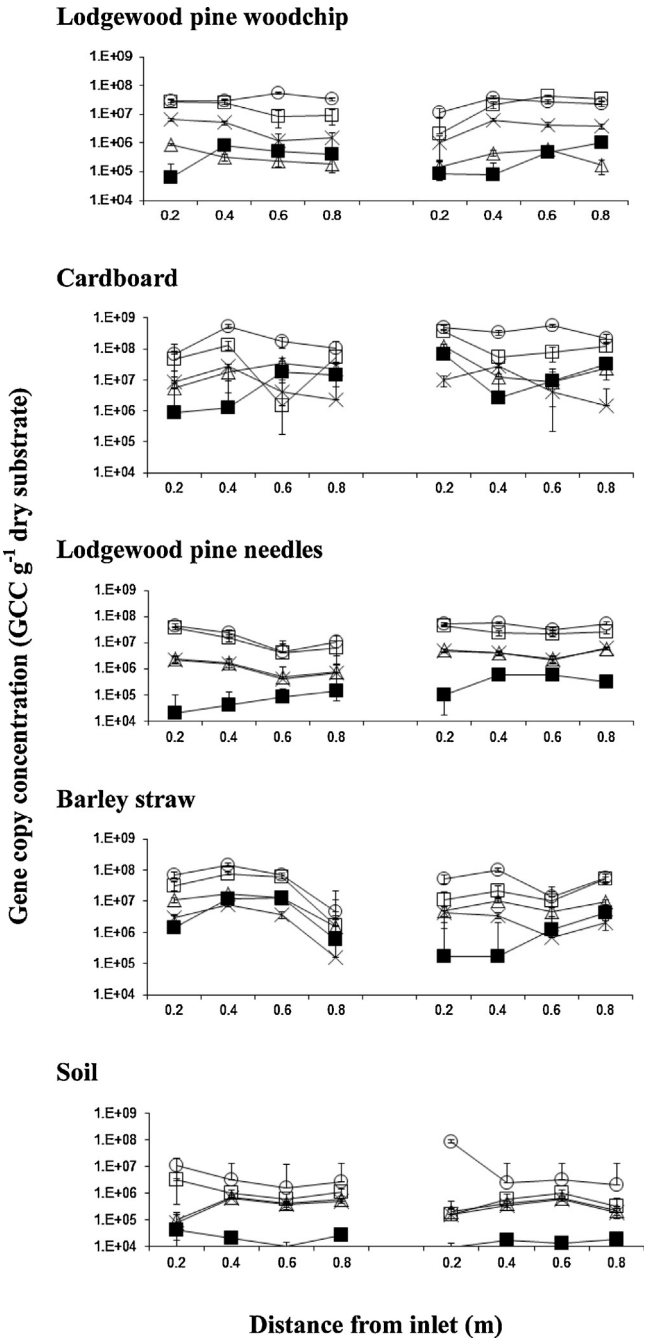

Fig. 11. Variation in gene copy concentration (GCC) of *nirK* (open triangle), *nirS* (open square), *nosZ* (cross hairs) and archaeal (closed square), and bacterial 16S rRNA (open circle) obtained from sampling ports located at distances of 0.2, 0.4, 0.6 and 0.8 m from the base in two arbitrary sets of lodgewood pine woodchip, cardboard, lodgepole pine needles, barley straw and soil-only bioreactors (NTC undetected for each respective assay). Standard errors are indicated for each separate Q-PCR subgroup ($n = 3$).

sampling ports and the outlet was in the optimal range for denitrifiers (pH 7–8; Tchobanoglous et al., 2003). The inverse relationship between the HRT and NO_3^--N removal rate, combined with the lack of a discernible trend in nitrite reductase genes along the bioreactors (Fig. 11), suggests that, with the exception of LPW bioreactors, a shorter HRT would not have any adverse impact on performance. These findings are, however, very specific to this study. In field-scale bioreactors, HLR is very difficult to control, so bioreactors should be designed so that they have an adequate HRT for the effective reduction of NO_3^-.

4.2. Denitrifying bacterial communities

The CCB bioreactors had the greatest average abundance of denitrification genes but lowest number of dentrification genes as a proportion of total bacteria and the highest number of 16S rRNA GCC g^{-1}. Excluding the control bioreactors, the other bioreactors (BBS, LPN and LPW) had a similar number of denitrification genes and total bacterial DNA, and both parameters were at least an order of magnitude less than the cardboard bioreactors. The LPN and LPW bioreactors had the highest number of dentrification genes as a proportion of total bacteria. This implies that a greater proportion of C in cardboard bioreactors was consumed by non-dentrifying bacteria, fungi or yeasts, whereas a greater proportion of C in the LPN and LPW bioreactors was consumed by denitrifiers. In order to verify this, further work would be necessary targeting alternative stains. The fact that a greater proportion of denitrifiers were present in the LPN/LPW media coincided with higher N_2O emissions, which were observed in both media at the highest loading rate. This increase in N_2O level also coincided with a decrease in the efficiency of NO_3^- removal at the highest loading rate. It may indicate either partial denitrification to N_2O *in situ* or degassing of dissolved N_2O in the original water in the column.

The ratio of *nirS*/*nirK* and total number of nitrite reductase genes (Σ*nir*)/*nosZ* was similar between replicate bioreactors and within each 0.2-m-depth in every bioreactor. There was no indication that populations of denitrifying or non-denitrifying bacteria were grouped at any particular point within the bioreactors (i.e., toward the inlet or outlet). The nutrient concentrations measured at each 0.2-m-depth increment were consistent with this finding (Figs. 5 and 7). There appears to be a greater variation in denitrifying gene number and presence between the reactors than within an individual reactor, based on the sampling resolution used. Indicating microbial populations and activity established in each bioreactor, therefore, reflect and respond to the nature of the media therein (and microbial evolution of the system), as opposed to operation of the bioreactor (i.e., HRT). Overall, this suggests that gene analysis may be employed to reliably assess the relative dominance of the denitrifying microbial populations. Further work is necessary to determine if it could be used as a potential proxy for bioreactor design and optimisation.

4.3. Greenhouse gases

Anoxic to anaerobic conditions in the bioreactors resulted in high levels of CH_4 efflux and relatively low CO_2 and N_2O loss. Anaerobic conditions result in the complete denitrification of nitrite and subsequently nitrate to N_2. As a result, the N_2O flux in the bioreactors was very low and negative fluxes were observed in some cases; in these instances, *nir* GCCs were lower than *nosZ* GCCs. A significant flux was only observed at higher HLRs, where the presence of dissolved O_2 in the influent may allow some partial denitrification to N_2O. This, combined with the higher pressures in the system, may subsequently result in the degassing of dissolved N_2O, and coincided with decreased nitrate removal from the bioreactors.

Apart from the cardboard medium, CO_2 release from heterotrophic respiration was very low compared with normal rates of (7–30 g CO_2 m^{-2} d^{-1}) of soil respiration (Lloyd and Taylor, 1994). The higher rate of CO_2 and CH_4 efflux in the cardboard bioreactors reflected the successional mobilisation of organic C *via* heterotrophic and anaerobic respiration, and was also related to the archael 16S rRNA GCC abundance. Carbon within the media was utilised principally by denitrifying bacteria, generating CO_2 that was either directly emitted or consumed by methanogens as the terminal electron acceptor in methanogenesis (Wolin and Miller, 1987). The lower rates observed in LPW, LPN and CSO bioreactors (0.02 mg

Table 3
Net fluxes (in g m^{-2} d^{-1}) ± standard deviations (in brackets) of major dissolved compounds and greenhouse gases (expressed as CO_2 equivalents per unit surface area per day) from laboratory scale denitrifying bioreactors, operated at steady-state, for the three hydraulic loading rates (HLRs), 3, 5, and 10 cm d^{-1}. Negative and positive fluxes indicate remediation and production of the compound, respectively.

HLR (cm d^{-1})	Media[a]	NO_3^--N	NH_4^+-N	PO_4^{3-}-P	CH_4	CO_2	N_2O
3	LPW	−0.81 (0)	0.11 (0.01)	0.003 (0)	4.01 (2.04)	3.86 (1.04)	0.57 (0.39)
	Cardboard	−0.60 (0)	0.05 (0.01)	0.001 (0)	296.03 (26.67)	21.04 (4.41)	0.04 (0.03)
	LPN	−0.78 (0)	0.05 (0.02)	0.000 (0)	2.52 (1.26)	5.13 (1.85)	0.10 (0.04)
	BBS	−0.75 (0)	0.03 (0.01)	0.001 (0)	100.29 (55.69)	8.26 (1.35)	0.22 (0.08)
–							
5	LPW	−1.00 (0.1)	0.03 (0)	0.018 (0.013)	11.57 (2.29)	1.51 (0.37)	1.48 (1.09)
	Cardboard	−1.09 (0)	0.03 (0.02)	0.001 (0)	99.43 (35.48)	6.88 (3.73)	0.02 (0.04)
	LPN	−1.08 (0)	0.03 (0)	0.002 (0)	0.70 (0.55)	1.38 (0.57)	0.09 (0.70)
	BBS	−1.08 (0)	0.02 (0)	0.001 (0)	38.04 (18.57)	3.10 (0.50)	0.13 (0.09)
–							
10	LPW	−1.46 (0.24)	0.07 (0.03)	0.003 (0.001)	0 (0.01)	1.47 (0.34)	3.29 (2.88)
	Cardboard	−2.15 (0)	0.05 (0.03)	0.002 (0)	85.36 (23.19)	6.12 (2.33)	0.69 (0.78)
	LPN	−2.19 (0)	0.06 (0.01)	0.003 (0.002)	3.71 (1.47)	1.66 (0.65)	4.11 (3.28)
	BBS	−2.12 (0)	0.03 (0)	0 (0)	4.28 (1.84)	1.42 (0.69)	0.02 (0.12)

[a] LPW = lodgepole pine woodchips; LPN = lodgewood pine needles; and BBS = barley straw.

CH_4 m^{-2} d^{-1} to 0.34 mg CH_4 m^{-2} d^{-1} for soil and LPW bioreactors, respectively) were comparable to typical values of diffusional (non-ebullition) methane fluxes from peatlands, which range from 1.5 to 480 mg CH_4 m^{-2} d^{-1} (Coulthard et al., 2009). The higher rates in the cardboard (8.8 mg CH_4 m^{-2} d^{-1}) and, to a lesser extent, BBS bioreactors (3 mg CH_4 m^{-2} d^{-1}), reflect higher rates of microbial activity presumably due to more labile C sources. Emissions from both these media were greatest at the lowest loading rates (2.5–8.8 g CH_4-C m^{-2} d^{-1}), equating to an annual methane loss of between 1.3 and 4.3 kg CH_4 m^{-2} yr^{-1}. These emissions are similar to localised methane ebullition from peatlands, where fluxes can range from 1.2 to 26 g CH_4-C m^{-2} d^{-1} (Glaser et al., 2004; Tokida et al., 2007).

The high total GHG emissions from CCB and BBS bioreactors were dominated by methane and were 50 times higher than other media, which had comparable or better nitrate removal. As such, these media should be avoided in bioreactors or if they are used, some form of remedial action, such as soil capping, should be utilised to oxidise some of the methane and reduce this flux to the atmosphere (Stern et al., 2007).

4.4. Identification of optimum loading rates considering pollution swapping

The net flux of each parameter of interest in this study is shown in Table 3 and the SI calculations for three scenarios (1 = only NO_3^- considered; 2 = all mixed contaminants in water; and 3 = water and gaseous emissions) are presented in Table 4. For scenario 1, LPW bioreactors performed best at the lowest HLR, and cardboard and LPN bioreactors performed best at the two higher HLRs. In scenario 2, BBS bioreactors had the best performance across all HLRs. In scenario 3, LPN bioreactors performed best at HLRs of 3 and 5 cm d^{-1}, whereas LPW bioreactors performed best at a HLR of 10 cm d^{-1}. Considering all water quality and gaseous parameters for the three scenarios, analysed at each HLR, the LPN bioreactors performed best. However, there was an 80% reduction in TC from the LPN bioreactors over its operation period (approximately 560 days) (Fig. 2). In comparison, the LPW bioreactors only experienced a TC loss of approximately 27% over 745 days of operation, which suggests this type of bioreactor may have greater longevity than LPN bioreactors.

It is important for research to start moving from single contaminant to mixed contaminant mitigation, as conceptualised by Fenton et al. (2014). The type of analysis conducted in this study is considerably simplified, but highlights the huge disadvantages of the single contaminant approach. In reality, attributing weighting factors to both dissolved contaminants and GHGs would be considerably more complex, and require consideration of their respective costs and benefits, local legislation and environmental conditions, as well as cognisance of the fact that legislation will change over time. If total removal of mixed contaminants, apart from achievement of maximum admissible concentrations or

Table 4
Net flux (g m^{-2} d^{-1}) and sustainability index (SI) calculations, calculated from Table 2, for the filter media for three scenarios (see text for explanation). Negative and positive net fluxes indicate removal and production of the compound, respectively. A high SI indicates poor performance, a low SI indicates good performance.

HLR (cm d^{-1})	Media[a]	Scenario 1 Net flux (g m^{-2} d^{-1})	SI	Scenario 2 Net flux (g m^{-2} d^{-1})	SI	Scenario 3 Net flux (g m^{-2} d^{-1})	SI	Overall ranking[b]
3	LPW	−0.81	1	0.06	3	7.74	2	7
	Cardboard	−0.60	4	0.03	4	316.56	4	11
	LPN	−0.78	2	0.02	1	7.02	1	5
	BBS	−0.75	3	0.01	2	108.05	3	7
–								
5	LPW	−1.00	3	0.03	3	13.61	2	7
	Cardboard	−1.09	1	0.01	1	105.27	4	6
	LPN	−1.08	2	0.01	2	1.12	1	4
	BBS	−1.08	2	0.01	1	40.21	3	6
–								
10	LPW	−1.46	4	0.03	4	3.37	1	8
	Cardboard	−2.15	2	0.02	2	90.07	4	8
	LPN	−2.19	1	0.03	1	7.35	3	7
	BBS	−2.12	3	0.01	3	3.63	2	6

[a] LPW = lodgewood pine woodchips; LPN = lodgewood pine needles; and BBS = barley straw.
[b] Obtained from the sum of the sustainability indices (SIs) for each scenario.

targets, is the goal, more efficient systems will need to be envisaged for the future. The co-location of denitrifying bioreactor and adsorption structures in sequence – termed "permeable reactive interceptors" – is a move in this direction (Fenton et al., 2014).

5. Conclusions

The way in which the performance of denitrifying bioreactors is assessed can lead to different conclusions about optimum HRT and media selection. When NO_3^- removal only was assessed (single contaminant approach), there was a net removal in all bioreactors, which increased as HRT reduced. All bioreactors performed best at HRTs of around 5 days. When all contaminants (NO_3^-, NH_4^+ and PO_4^{3-}) were considered, there was a net flux of contaminants from all columns, which further increased when greenhouse gas emissions were also considered. To reduce pollution swapping from bioreactors, suitable media could be placed in sequence in the filters, which would be capable of reducing the contaminant of interest before final discharge. Based on the study results, LPN bioreactors appeared to be the most effective design, across all HRTs and scenarios, at effectively treating NO_3^-, while limiting pollution swapping. However, a substantial amount of carbon was lost over a relatively short period (around 80% of the initial content of the LPN bioreactors). This indicates that a more commonly available filter media, such as LPW, may be more suitable for the long-term operation of bioreactors.

Microbiological testing of the filter media at the end of the experiment indicated that denitrification was most likely the main mechanism for NO_3^--N removal and that there was no clustering of the denitrifying or non-denitrifying bacteria at any particular point within the bioreactors. The addition of carbon appeared to affect the abundance of denitrifiers possessing the targeted functional genes. Moreover, the cardboard bioreactor contained the highest abundance of denitrifying microorganisms compared with the other bioreactors, indicating that the source of carbon influenced the abundance of denitrifying microbes. Microbiological analyses, such as those performed in this study, could be used as a proxy for system performance at various HRTs with further testing. However, this analysis could not be performed in the current study, as the microbiological testing was conducted in the columns having been subjected to three HLRs.

Acknowledgement

This study was funded by the Department of Agriculture, Food and Marine under the Research Stimulus Programme 2007 (RSF 07 525).

References

APHA, 1995. Standard Methods for Examination of Water and Wastewater, 19th ed. American Public Health Association, Washington, DC.

Barrett, M., Jahangir, M.M.R., Lee, C., Smith, C.J., Bhreathnach, N., Collins, G., Richards, K.G., O'Flaherty, V., 2013. Abundance of denitrification genes under different piezometer depths in four agricultural groundwater sites. Environ. Sci. Pollut. Res. 20 (9), 6646–6657.

Braker, G., Fesefeldt, A., Witzel, K.P., 1998. Development of PCR primer systems for amplification of nitrite reductase genes (nirK and nirS) to detect denitrifying bacteria in environmental samples. Appl. Environ. Microbiol. 64 (10), 3769–3775.

Cameron, S.G., Schipper, L.A., 2010. Nitrate removal and hydraulic performance of organic carbon for use in denitrification beds. Ecol. Eng. 36 (11), 1588–1595.

Christianson, L.E., Bhandari, A., Helmers, M.J., 2011. Pilot-scale evaluation of denitrification drainage bioreactors: reactor geometry and performance. ASCE J. Environ. Eng. 137 (4), 213–220.

Chun, J.A., Cooke, R.A., Eheart, J.W., Kang, M.S., 2009. Estimation of flow and transport parameters for woodchip-based bioreactors: I. laboratory-scale bioreactor. Biosystems Eng. 104 (3), 384–395.

Clarke, K.R., Somerfield, P.J., Chapman, M.G., 2006. On resemblance measures for ecological studies, including taxonomic dissimilarities and a zero-adjusted Bray–Curtis coefficient for denuded assemblages. J. Exp. Mar. Biol. Ecol. 330 (1), 55–80.

Coulthard, T.J., Baird, A.J., Ramirez, J., Waddington, J.M., 2009. Methane dynamics in peat: importance of shallow peats and a novel reduced-complexity approach for modeling ebullition. In: Baird, A.J., Belyea, L.R., Comas, X., Reeve, A.S., Slater, L.D. (Eds.), Carbon Cycling in Northern Peatlands. American Geophysical Union, Washington.

Durand, P., Breuer, L., Johnes, P.J., 2011. Nitrogen processes in aquatic ecosystems. In: Sutton, M.A., Howard, C.M., Erisman, J.W., Billen, G., Bleeker, A., Grennfelt, P., van Grinsven, H., Grizzetti, B. (Eds.), The European Nitrogen Assessment-Sources, Effects and Policy Perspectives. Cambridge University Press, Cambridge, pp. 126–146.

Elgood, Z., Robertson, W.D., Schiff, S.L., Elgood, R., 2010. Nitrate removal and greenhouse gas production in a stream-bed denitrifying bioreactor. Ecol. Eng. 36 (11), 1575–1580.

Fenton, O., Richards, K.G., Kirwan, L., Healy, M.G., 2009. Factors affecting nitrate distribution in shallow groundwater using a beef farm in south eastern Ireland. J. Environ. Manage. 90 (10), 3135–3146.

Fenton, O., Schulte, R.P.O., Jordan, P., Lalor, S., Richards, K.G., 2011. Time lag: a methodology for the estimation of vertical and horizontal travel and flushing timescales to nitrate threshold concentrations in Irish aquifers. Environ. Sci. Policy 14 (4), 419–431.

Fenton, O., Healy, M.G., Brennan, F., Jahangir, M.M.R., Lanigan, G.J., Richards, K.G., Thornton, S.F., Ibrahim, T.G., 2014. Permeable reactive interceptors: blocking diffuse nutrient and greenhouse gases losses in key areas of the farming landscape. J. Agric. Sci doi:http://dx.doi.org/10.1017/S0021859613000944 Available on CJO2014.

Flechard, C.R., Nemitz, E., Smith, R.I., Fowler, D., Vermeulen, A.T., Bleeker, A., Erisman, J.W., Simpson, D., Zhang, L., Tang, Y.S., Sutton, M.A., 2011. Dry deposition of reactive nitrogen to European ecosystems: a comparison of inferential models across the NitroEurope network. Atmos. Chem. Phys. 11 (6), 2703–2728.

Fujinuma, R., Venterea, R.T., Ranaivoson, A., Moncrief, J., Dittrich, M., 2011. On-site wood-chip bioreactors could reduce indirect nitrous oxide emissions from tile drain waters. Proceedings of Nutrient Efficiency and Management Conference, MN Department of Agriculture, Minnesota, February, 2011.

Glaser, P.H., Chanton, J.P., Morin, P., Rosenberry, D.O., Siegel, D.I., Ruud, O., Chasar, L.I., Reeve, A.S., 2004. Surface deformations as indicators of deep ebullition fluxes in a large northern peatland. Global Biogeochem. Cycles 18 (1), 1–15.

Grennan, C.M., Moorman, T.B., Parkin, T.B., Kaspar, T.C., Jaynes, D.B., 2009. Denitrification in wood chip bioreactors at different water flows. J. Environ. Qual. 38 (4), 1664–1671.

Grizzetti, B., Bouraoui, F., Aloe, A., 2012. Changes in nitrogen and phosphorus loads to European seas. Global Change Biol. 18 (2), 769–782.

Healy, M.G., Rodgers, M., Mulqueen, J., 2006. Denitrification of a nitrate-rich synthetic wastewater using various wood-based media materials. J. Environ. Sci. Health, Part A 41 (5), 779–788.

Healy, M.G., Ibrahim, T.G., Lanigan, G.J., Serrenho, A.J., Fenton, O., 2012. Nitrate removal rate, efficiency and pollution swapping potential of different organic carbon media in laboratory denitrification bioreactors. Ecol. Eng. 40 (March), 198–209.

Henry, S., Bru, D., Stres, B., Hallet, S., Philippot, L., 2006. Quantitative detection of the *nosZ* gene, encoding nitrous oxiden reductase, and comparison of the abundances of 16S rRNA, *narG*, *nirK*, and *nosZ* genes in soils. Appl. Environ. Microbiol. 72 (8), 5181–5189.

Henze, M., Harremoes, P., Jansen, J.L.C., Arvin, E., 1997. Wastewater Treatment: Biological and Chemical Processes. Springer, Berlin.

Hutchinson, G.L., Mosier, A.R., 1981. Improved soil cover method for field measurement of nitrous oxide fluxes. Soil Sci. Soc. Am. J. 45 (2), 311–316.

IPCC, 2013. Climate change 2013: the physical science basis. Contribution of Working Group I to the fifth assessment report of the intergovernmental panel on climate change (Chapter 8), p. 714.

Kandeler, E., Deiglmayr, K., Tscherko, D., Bru, D., Philippot, L., 2006. Abundance of *narG*, *nirS*, *nirK*, and *nosZ* genes of denitrifying bacteria during primary successions of a glacier foreland. Appl. Environ. Microbiol. 72 (9), 5957–5962.

Lee, C., Kima, J., Hwang, K., O'Flaherty, V., Hwang, S., 2009. Quantitative analysis of methanogenic community dynamics in three anaerobic batch digesters treating different wastewaters. Water Res. 43 (1), 157–165.

Levenspiel, O., 1999. Chemical Reaction Engineering. John Wiley and Sons, New York.

Lloyd, J., Taylor, J.A., 1994. On the temperature dependence of soil respiration. Funct. Ecol. 8, 315–323.

Moorman, T.B., Parkin, T.B., Kaspar, T.C., Jaynes, D.B., 2010. Denitrification activity, wood loss, and N_2O emissions over 9 years from a wood chip bioreactor. Ecol. Eng. 36 (11), 1567–1574.

Richardson, D., Felgate, H., Watmough, N., Thomson, A., Baggs, E., 2009. Mitigating release of the potent greenhouse gas N_2O from the nitrogen cycle – could enzymic regulation hold the key? Trends Biotechnol. 27 (7), 388–397.

Rivett, M.O., Buss, S.R., Morgan, P., Smith, J.W., Bemment, C.D., 2008. Nitrate attenuation in groundwater: a review of biogeochemical controlling processes. Water Res. 42 (16), 4215–4232.

Robertson, W.D., 2010. Nitrate removal rates in woodchip media of varying age. Ecol. Eng. 36 (11), 1581–1587.

Schipper, L.A., Robertson, W.D., Gold, A.J., Jaynes, D.B., Cameron, S.C., 2010. Denitrifying bioreactors – an approach to reducing nitrate loads to receiving waters. Ecol. Eng. 36 (11), 1532–1543.
Schmidt, C.A., Clark, M.W., 2012. Efficacy of a denitrification wall to treat continuously high nitrate loads. Ecol. Eng. 42 (May), 203–211.
Schmidt, C.A., Clark, M.W., 2013. Deciphering and modelling the physiochemical drivers of denitrification rates in bioreactors. Ecol. Eng. 60, 276–288.
Stern, J.C., Chanton, J., Abichou, T., Powelson, D., Yuan, L., Escoriza, S., Bogner, J., 2007. Use of a biologically active cover to reduce landfill methane emissions and enhance methane oxidation. Waste Manage. 27 (9), 1248–1258.
Tchobanoglous, G., Burton, F.L., Stensel, H.D., 2003. Wastewater Engineering, Treatment and Reuse. McGraw Hill, New York, NY.
Tokida, T., Miyazaki, T., Mizoguchi, M., Nagata, O., Takakai, F., Kagemoto, A., Hatano, R., 2007. Falling atmospheric pressure as a trigger for methane ebullition from a peatland. Global Biogeochem. Cycles 21, GB2003.
Yu, Y., Lee, C., Kim, J., Hwang, S., 2005. Group-specific primer and probe sets to detect methanogenic communities using quantitative real-time polymerase chain reaction. Biotechnol. Bioeng. 89 (6), 670–679.
Warneke, S., Schipper, L.A., Bruesewitz, D.A., McDonald, I., Cameron, S., 2011a. Rates, controls and potential adverse effects of nitrate removal in a denitrification bed. Ecol. Eng. 37 (3), 511–522.
Warneke, S., Schipper, L.A., Matiasek, M.G., Scow, K.M., Cameron, S., Bruesewitz, D. A., McDonald, I.R., 2011b. Nitrate removal, communities of denitrifiers and adverse effects in different carbon substrates for use in denitrification beds. Water Res. 45 (17), 5463–5475.
Wolin, M.J., Miller, T.L., 1987. Bioconversion of organic carbon to CH_4 and CO_2. Geomicrobiology 5 (3–4), 239–259.
Xu, Z., Shao, L., Yin, H., Chu, H., Yao, Y., 2009. Biological dentrification using corncobs as a carbon source and biofilm carrier. Water Environ. Res. 81 (3), 242–247.